MULTIPLE-MEASUREMENT BEAM PROBE*

J. D. Gilpatrick and D. L. Grant, AT-8, MS H821
Los Alamos National Laboratory, Los Alamos, New Mexico 87545

Summary

Particle accelerators are becoming smaller and are producing more intense beams; therefore, it is critical that beam-diagnostic instrumentation provide accelerator operators and automated control systems with a complete set of beam information. Traditionally, these beam data were collected and processed using limited-bandwidth interceptive techniques. For the new-generation accelerators, we are developing a multiple-measurement microstrip probe to obtain broad-band beam data from inside a drift tube without perturbing the beam. The cylindrical probe's dimensions are 6-cm o.d. by 1.0 cm long, and the probe is mounted inside a drift tube. The probe (and its associated electronics) monitors bunched-beam current, energy, and transverse position by sensing the beam's electromagnetic fields through the annular opening in the drift tube. The electrical impedance is tightly controlled through the full length of the probe and transmission lines to maintain beam-induced signal fidelity. The probe's small, cylindrical structure is matched to beam-bunch characteristics at specific beamline locations so that signal-to-noise ratios are optimized. Surrounding the probe, a mechanical structure attaches to the drift-tube interior and the quadrupole magnets; thus, the entire assembly's mechanical and electrical centers can be aligned and calibrated with respect to the rest of the linac.

Probe and Environment Constraints

Accelerator operators and automated control systems require more timely beam information as demands for increased particle-beam brightness occur. Also, as increased beam energy is required, traditional linac structures become longer and demand broad-band beam information from within the accelerator so that beam malfunctions can be precisely diagnosed or so that rapid automated corrections can be implemented. One possible area for noninterceptive beam-probe placement is inside a drift tube that has an annular portion of the bore removed. This geometry gives the probe clear access to the beam but restricts both probe materials and geometries. The measured beam parameters for initial acceleration operation are current, energy, and transverse position. After stable accelerator operation has been obtained, second-moment and phase-space information for all three cartesian coordinates is required.

All of these qualifications can be supplied by using a style of strip-line probe we call a microstrip electromagnetic probe. It is very similar to the classic 50-Ω strip-line probe being used in many other accelerator facilities except that it is much smaller and is loaded with an appropriate dielectric. The probe must be able to sense beams of $\beta > 0.046$, $J_{rms} \geq 5.0$ mA/cm^2, longitudinal bunch widths (five standard deviations) of one-sixth an rf period, and N (number of ions) $\geq 5 \times 10^6$ singly charged particles. Because the probe is open to the evacuated beam tube, the outgas rate must be small and the probe material must be insensitive to various, ionizing-radiation sources (especially at the high-energy end of the linac). The most stringent restriction is the amount of volume within the drift tube that the probe and its signal-carrying transmission line must fit into. For the present set of accelerators being designed at Los Alamos, this volume has a cylindrical shape of approximately 6-cm o.d. by 2-cm i.d. by 0.5 to 2.5 cm long.

Microstrip-Probe and Transmission-Line Description

The probe consists of a cylinder of polyimide material whose inside diameter is slightly larger than the expected bore of the drift tube. The probe's length corresponds to between two and four standard deviations of the phase distribution of the bunched beam. In the bore of the probe are four (or eight) copper strips whose azimuthal widths are selected so as to minimize the electromagnetic coupling between both neighboring and cross-bore microstrips. In the case for the first operational probes, the widths of the four strips subtended 45° of the bore diameter with gaps of the same width between them. On the downstream side of the cylinder are four (or eight) chip-resistor arrays whose values are selected to match the characteristic impedance of the probe (50 Ω). On the upstream side of the probe, a strip-line, transmission line is connected to the probe's microstrips. These transmission lines carry the signals out to coaxial SMA connectors.

Figure 1 shows a conceptual model of this probe (with a slightly different shaped probe bore) and the first bench test of the 50-Ω strip-line transmission line. The outside diameter of the polyimide cylinder is covered with a layer of copper to provide a ground plane for the beam-induced signals on the copper microstrips. The copper on the polyimide cylinder was ion-beam, vapor deposited to a thickness of at least three times the skin depth at the fundamental rf frequency. The azimuthal-width/polyimide-thickness (w/h) microstrip ratios were selected to match electrical impedances of the connecting transmission lines. Given that the polyimide dielectric constant is 3.55, Edwards[1] suggested a w/h = 1.6 for 50-Ω impedances. Outside the probe's ground plane is another insulating material that attaches the probe to the permanent, split-quadrupole[2] magnets. This mechanical structure provides accurate alignment of the microstrip probe and electrically isolates the probe's ground plane from beamline ground.

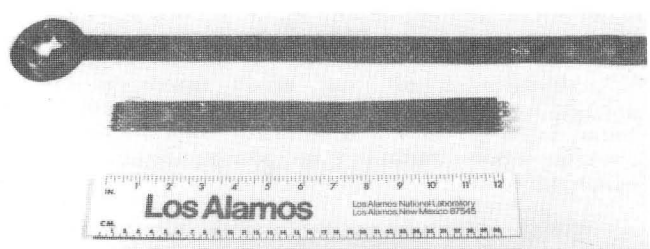

Fig. 1. The microstrip probe model (shown at top) depicts the polyimide cylinder attached to the strip-line transmission line. The lower device is the first bench-test version of the strip-line transmission line.

Figure 2 shows a cross section of the layers in the strip-line cable with an SMA connector being placed in the cable. The copper strips sandwiched

*Work performed under the auspices of the U.S. Dept. of Energy and supported by the U.S. Army Strategic Defense Command.

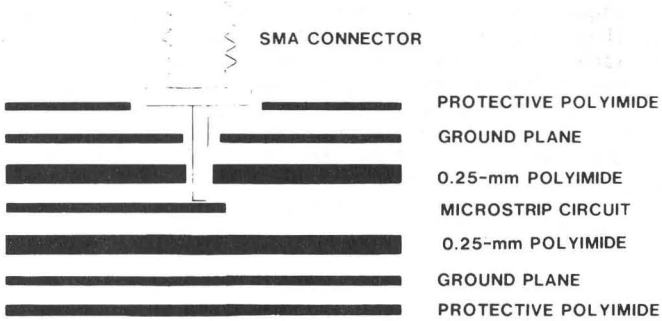

Fig. 2. The SMA connector (pictured above) penetrates one of the polyimide dielectric layers and is soldered to the microstrip layer.

between the 0.25-mm layers of sheet polyimide are 0.20 mm wide (calculated width). The full thickness of the transmission line is approximately 0.64 mm. The thin insulative polyimide layer on the outside of the cable isolates the signal's ground plane from beamline ground. The isolation is necessary because there is always noise--usually the accelerator-drive frequency is the largest component--on beamline ground near intense, rf-driven accelerators. Figure 3 shows the first manufactured test cable and its middle strip-line layer. The two sets of patterns etched on the middle layer are one single line progressing through five increasing discrete widths and four 0.2-mm-thick lines with 0.76, 1.5, and 2.29 mm between each line. These patterns allowed us to check transmission-line impedance and crosstalk.

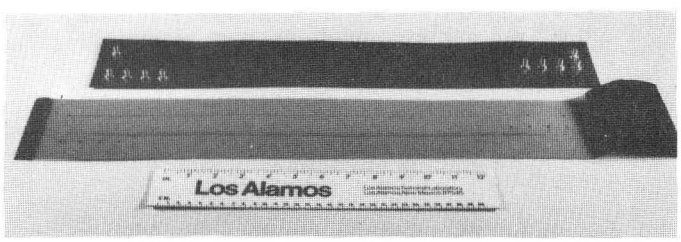

Fig. 3. The first strip-line transmission line and its microstrip layer, manufactured at Los Alamos.

Electrical Model

Figure 4 depicts an electrical model for the microstrip probe. The solid lines show a simplified, lumped-circuit model of each microstrip (components L_P and C_P); R_S is the measured dc resistance of the flat strip-line cable and R_T is the terminating resistance. The broken lines represent the coupling capacitances between neighboring (C_N) and opposite (C_O) strips; I_W^* is the beam's image current on each microstrip. This image current, Eq. (1), is an adaptation to Eq. (27) in Ref. 3. Here L is the length of the microstrips, and Φ_O is the azimuthal angle subtended by each microstrip:

$$I_w^*(\omega) = \frac{\Phi_o}{2\pi}\frac{dq(\omega,L)}{dt} \quad . \qquad (1)$$

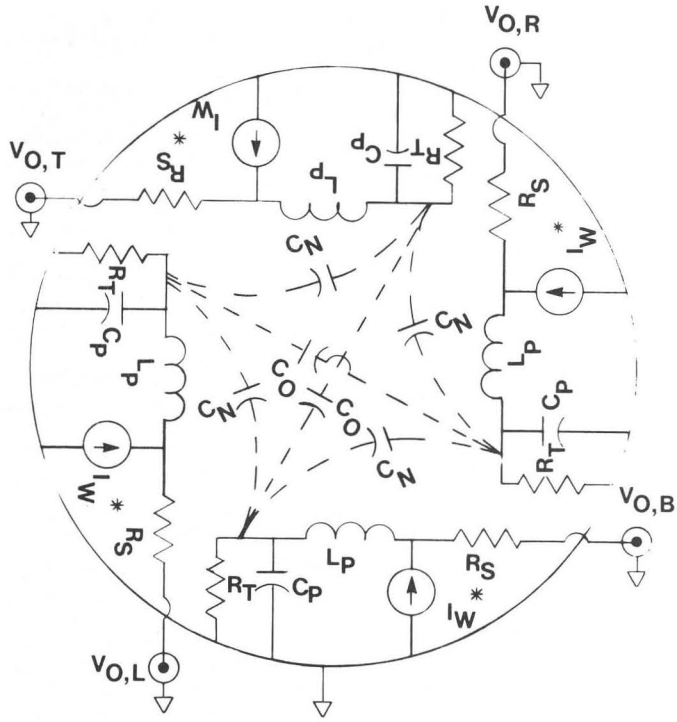

Fig. 4. The proposed electrical model of the microstrip probe includes neighboring and opposite microstrip coupling capacitances (C_N and C_O).

The transfer function for the probe is

$$\frac{V_O}{I_w^*}(j\omega) = Z_O \frac{\omega^2 - j\omega\frac{1}{C_P R_T} - \frac{1}{L_P C_P}}{\omega^2 - j\omega\left(\frac{1}{C_P R_T} + \frac{R_S + Z_O}{L_P}\right) - \frac{R_S + R_T + Z_O}{R_T C_P L_P}} \qquad (2)$$

where

$$C_P = \frac{L}{c\sqrt{\varepsilon}_R Z_O} \quad , \qquad (3)$$

$$L_P = \frac{L\sqrt{\varepsilon}_R Z_O}{c} \quad , \qquad (4)$$

and

c is the speed of light, ε_R is the relative dielectric constant, and $R_T = Z_O = 50\ \Omega$.

Signal Processing

Using SMA coaxial vacuum feedthroughs, the four signal transmission lines penetrate the vacuum wall of the beamline and are brought out a short distance (<3 m) to a passive preprocessing circuit. The signal information from these four coax cables is then processed and unfolded into ten separate signals. These output signals include the following:

(1) Broad-band signal composed of four added microstrip signals for integrated beam-current measurement

(2) Narrow-filtered signal composed of four added microstrip-signals for a time-of-flight beam-energy measurement

(3) Four separate signals whose phase differences represent signal amplitude difference of opposite microstrips
(4) Two separate signals that represent the amplitude sum of opposite microstrip signals
(5) Two separate signals that represent the amplitude difference between opposite microstrip signals

Signals, as described in Item 3 above, will be used for detecting beam position using ratios of opposite microstrip signals.[4] Other signals (Items 1, 4, and 5 above) will provide second moments in all three cartesian coordinates.[5,6] All four of the input cables to the preprocessing circuitry are phase matched so that errors in length do not result in phase errors in the position measurement. The post-processing active circuitry (which is currently being designed) will reside outside the accelerator vault in crates and racks, which will give personnel easy access to rf-signal sources and electronics.

Transmission-Line Data

Figure 5 shows a time-domain-reflectometer measurement of the stepped-width line in the transmission line of Fig. 3. The trace shows a 50-Ω impedance (far right in Fig. 5), dropping from the SMA connector to a 0.305-mm strip-line width and traveling through (and to the left, Fig. 5) five distinct steps to a 0.102-mm strip-line width. The 0.23-mm strip-line impedance (Fig. 5.) near horizontal center is close to the 0.20-mm calculated width for a 50-Ω impedance. We

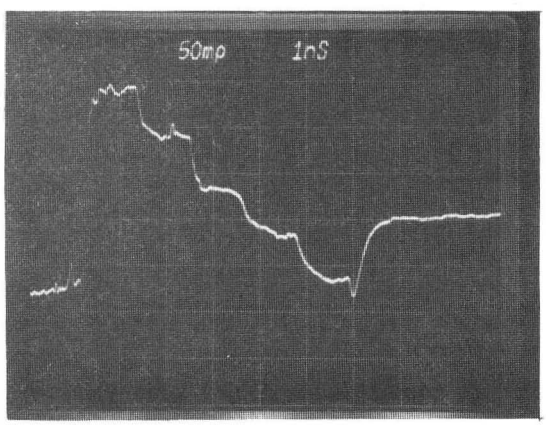

Fig. 5. A time-domain reflectometer response to the stepped-width line in the stripline transmission line shows the 50-Ω impedance line width of approximately 0.23 mm.

believe that the epoxy adhesives used to bond the layered cable altered the bulk dielectric constant and increased the cable impedance. The series resistance of the four 0.20-mm-thick lines was 2.1 Ω. The cross-sectional area for the final cable design should be at least 15% larger; thus, the series dc resistance should be approximately 1.8 Ω. This resistance will give a VSWR of 1.07:1, which is more than adequate for frequencies below 4.0 Ghz. To measure crosstalk, we connected a 425-MHz, +10 dBm signal source to one of the four 0.20-mm terminated lines and measured the signal power on the adjacent line. These data were then compared to several RG-178 coax cables under the same signal-source conditions whose grounds were common. From the smallest to the largest spacing between lines, the coupled signal strengths were -36.2, -41, -47 dBm as compared to the -47-dBm signal power from the coax cables. These crosstalk data demonstrate that we can put at least four broad-band transmission lines within the 1.27-cm maximum cable width required for the specific, drift-tube application.

Conclusion

We have introduced a variation to the standard, strip-line noninterceptive probe for charged-particle beam detection. This probe's attraction is its small volume, well-defined electrical impedance, and flexible strip-line transmission line. We have discussed the strip-line transmission line and have proved its electrical feasibility. In the future, we intend to send several versions of the probe assembly to Argonne National Laboratory for measurement of the probe's frequency response.[7]

Acknowledgments

The authors gratefully acknowledge Bob Shafer and Ed Higgins for their intuitive discussions and Bill Powell for his innovative transmission-line construction.

References

1. T. C. Edwards, in Foundations for Microstrip Circuit Design (John Wiley & Sons, Inc., New York, 1981), Chap. 3.

2. D. J. Liska, "Thermal Design of Drift Tubes for High-Gradient Linacs," these proceedings.

3. J. H. Cuperus, "Monitoring of Particle Beams at High Frequencies," Nucl. Instrum. & Methods 145, 219 (1977).

4. E. F. Higgins and F. D. Wells, "A Beam Position Monitor System for the Proton Storage Ring at LAMPF," IEEE Trans. Nucl. Sci. 28 (3), 2308 (1981).

5. J. D. Gilpatrick and C. Watson, "Reconstruction of Longitudinal Beam Profiles from Nondestructive Electromagnetic Probes," IEEE Trans. Nucl. Sci. 32 (5), 1965 (1985).

6. R. H. Miller, "Nonintercepting Emittance Monitor," Proceedings of the 12th International Conference on High-Energy Accelerators, Fermilab National Accelerator Laboratory report, 602 (1983).

7. S. L. Kramer, "Relativistic Beam Pickup Facility," in Proceedings of the 12th International Conference on High-Energy Accelerators, Fermilab National Accelerator Laboratory report, 258-261 (1983).